

Systematics of pre- and near-scission α -particle multiplicities in heavy-ion-induced fusion-fission reactions

Y. K. Gupta,* D. C. Biswas, R. K. Choudhury, A. Saxena, B. K. Nayak, Bency John, K. Ramachandran, R. G. Thomas, L. S. Danu, B. N. Joshi, K. Mahata, S. K. Pandit, and A. Chatterjee

Nuclear Physics Division, Bhabha Atomic Research Centre, Mumbai 400 085, India

(Received 30 June 2011; published 20 September 2011)

The α -particle energy spectra have been measured in coincidence with fission fragments over a wide range of relative angles with respect to fragment emission direction in the ^{11}B (62 MeV) + ^{232}Th reaction. The α -particle multiplicity spectra have been fitted with moving source model to extract the prescission (α_{pre}) and near-scission (α_{nse}) components. The present results, along with available data from the literature over a wide range of Z^2/A and the excitation energy of a compound system, have been analyzed to develop certain global features of the pre- and near-scission emission characteristics. It is seen that α_{pre} values when normalized to $E_{\text{CN}}^{2,3}$ (E_{CN} is the compound nucleus excitation energy) show a systematic linearly increasing trend with the α -particle emission Q value (Q_α). The fraction of near-scission multiplicity is observed to be nearly the same at around 10% of the total prescission multiplicity for all the systems.

DOI: [10.1103/PhysRevC.84.031603](https://doi.org/10.1103/PhysRevC.84.031603)

PACS number(s): 25.85.-w, 25.70.Jj, 24.75.+i

In heavy-ion-induced fusion-fission reactions, neutron and charged-particle (mainly proton and α -particle) emission take place from various stages, namely from the fissioning compound nucleus (prescission) and from the accelerated fission fragments (postsission) [1,2]. Prescission neutron and charged-particle emission spectra and multiplicities provide important information on the statistical and dynamical aspects of the fusion-fission process [1,2]. The prescission neutron multiplicity, ν_{pre} has been shown to have a linearly increasing dependence on the compound nucleus excitation energy (E_{CN}) [3,4], whereas prescission charged-particle multiplicities increase nonlinearly with E_{CN} [3,5]. In the case of α -particle emission, it is observed that particles are also emitted very near the neck region in the fission process just before scission, akin to the ternary fission events in low-energy fission [6–10]. This part of prescission α particles emitted near the neck region is termed as near-scission emission (NSE). Although there have been many studies on prescission α -particle emission in many heavy-ion-induced fusion-fission reactions [1,2,5–9], a global systematics is yet to be developed. In low-energy fission (thermal neutron-induced, photo-, and spontaneous fission) NSE is a dominant channel [11–13] and exhibits characteristic energy and angular distributions corresponding to strong focusing of the particles by the Coulomb field of the fragments. The near-scission α -particle multiplicities are found to increase linearly with Z^2/A of the fissioning nucleus [11,12]. The features of the NSE observed in low-energy fission have been understood qualitatively with the sudden neck collapse dynamic model suggested by Halpern [13]. However, the validity of such a model has not been proven at elevated excitation energies and over a wide range of Z^2/A of fissioning nuclei typically encountered in heavy-ion-induced fusion-fission reactions. On the contrary, a statistical emission mechanism for the prescission α -particle emission, including the NSE part, has been suggested [14]. The study of

near-scission emission of α particles can provide information on the scission point characteristics of the fissioning nucleus and is important from the point of understanding the collective fission dynamics. There are no systematic studies so far for the NSE over a large fissility (x) range in heavy-ion-induced fusion-fission reactions.

In the present work, we have carried out measurements of α -particle energy spectra in coincidence with fission fragments for the system ^{11}B (62 MeV) + ^{232}Th ($Z^2/A = 37.13$, $x = 0.798$) in a wide range of relative angles between fission fragments and α particles. The α -particle multiplicity spectra at various relative angles have been fitted simultaneously with the moving source model calculations to extract the components of multiplicity corresponding to emission at different stages of the fusion-fission process. The present results are analyzed along with data from literature over a wide range of excitation energy and fissility of the compound system to develop systematic features of pre- and near-scission emission as a function of α -particle emission Q value and Z^2/A of compound systems.

Experiments were performed using a ^{11}B beam of energy 62 MeV from the BARC-TIFR 14-MV Pelletron accelerator facility at Mumbai. A self-supporting thin metallic foil of ^{232}Th of thickness 1.6 mg/cm² was used as the target. Measurements were carried out in two separate experiments. In the first experiment, the fission fragments were detected using a position sensitive 32-strip silicon detector (SSD) having delay line read-out [15] with an angular opening of $\sim 32^\circ$ and centered at 150° with respect to the beam direction. In the second experiment, a position sensitive gridded gas ionization chamber consisting of ΔE_{gas} and E_{gas} elements [16] was used to detect fission fragments. The detector was centered at 145° with respect to beam direction and covered an angular opening of 30° . In both the experiments, α particles were detected by three collimated CsI(Tl)-Si(PIN) detectors [17] with an angular opening of $\pm 3.5^\circ$. The particle identification in CsI(Tl) detectors was achieved using pulse shape discrimination (zero cross over) technique. The energy threshold for α -particle

* ykgupta@barc.gov.in

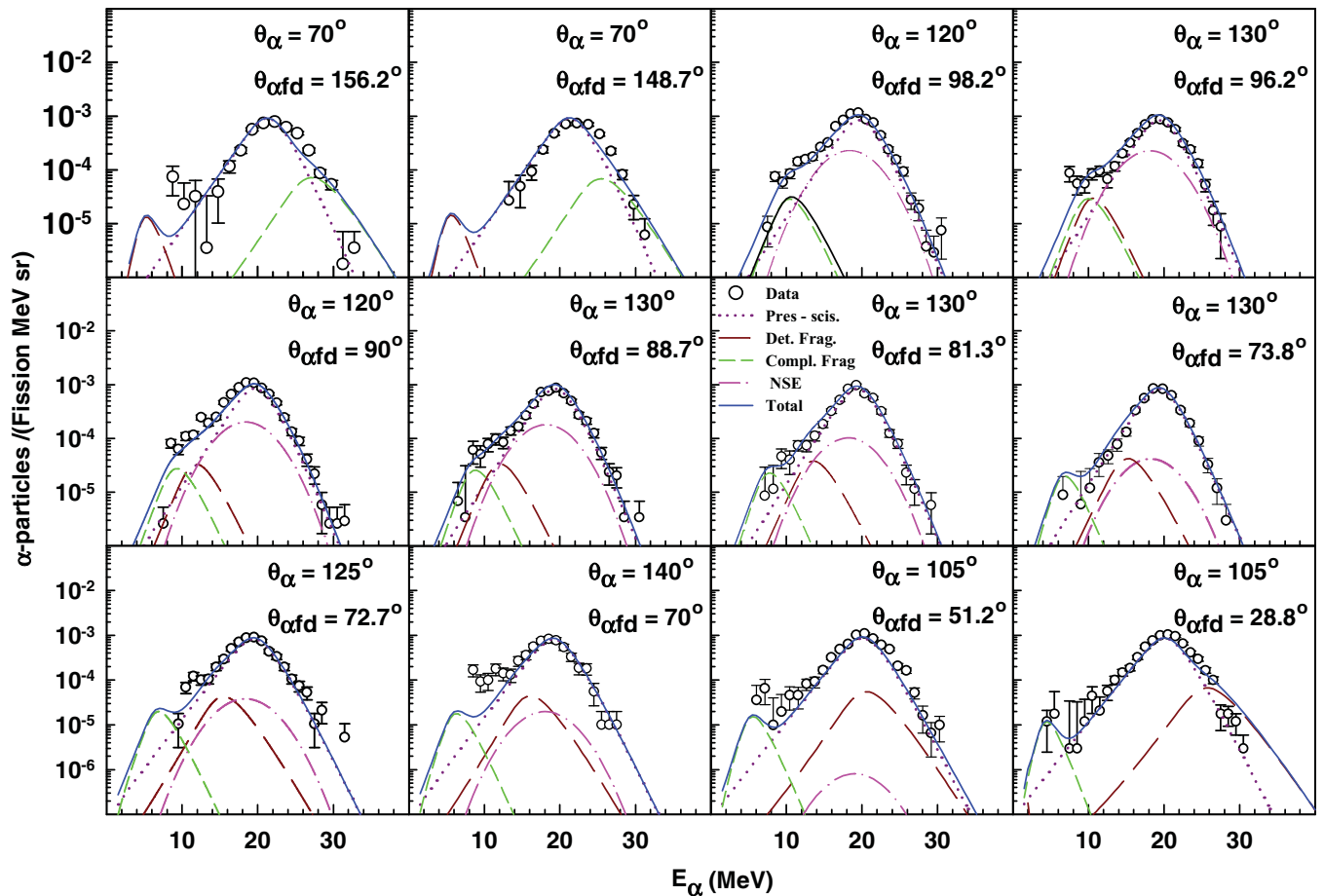


FIG. 1. (Color online) The α -particle multiplicity spectra along with fits of moving source model for different combination of laboratory angles of CsI(Tl) detectors with respect to beam direction, θ_α , and detected fission fragments, $\theta_{\alpha fd}$. The solid curve indicates total contribution from four sources. The dotted, long-dashed, short-dashed, and dash-dot curves are contributions from compound nucleus, detected fission fragment, complementary fission fragment, and near-scission emission, respectively.

identification was ~ 9.5 MeV (and ~ 5 MeV in the second experiment). The higher threshold in the first experiment is due to a $14.9\text{-}\mu\text{m}$ aluminum foil used to stop the fission fragments. The CsI(Tl) detectors were energy calibrated for α particles using $^{228,229}\text{Th}$ source and in-beam energy calibration runs. In the first experiment, the in-beam calibration made use of the discrete α -particle peaks corresponding to $^{15}\text{N}^*$ states from the reactions $^{12}\text{C} (^7\text{Li}, \alpha) ^{15}\text{N}^*$ at a ^7Li beam energy of 15 MeV. In the second experiment, the discrete states of $^{20}\text{Ne}^*$ from the $^{12}\text{C} (^{12}\text{C}, \alpha) ^{20}\text{Ne}^*$ reaction at ^{12}C beam energies of 25 and 40 MeV were used.

In the first experiment, the CsI(Tl) detectors were placed at the back angles in the range of 115° to 155° on either side of the beam direction. In the second experiment, the CsI(Tl) detectors were placed at angles of 70° , 130° , and 105° with respect to the beam direction. The angular opening of the fission detector in both the experiments was divided into four equal parts. Thus, a total number of 24 combinations of α -particle spectra, each having different relative angles with respect to the beam (θ_α) and fission fragments ($\theta_{\alpha fd}$), were obtained from the combined geometry of both the experiments. After correcting for random coincidence, the normalized α -particle

multiplicity spectra were obtained by dividing the coincidence spectra with total number of fission single events. Figure 1 shows typical normalized α -particle multiplicity spectra for 12 of 24 combinations of θ_α and $\theta_{\alpha fd}$.

These 24 multiplicity spectra are fitted simultaneously by the moving source model, including four different sources, namely the compound nucleus, the two complementary fission fragments, and the NSE. In the moving source analysis, symmetric mass division is assumed for the fragments and mean values of fragment mass and charge have been used. The α particles are assumed to be emitted isotropically in the rest frames of pre- and postscission sources. The α -particle energy spectra in the rest frames for pre- and postscission sources are calculated using the constant-temperature level-density formula with the expression [1,18];

$$n(\epsilon) = N\alpha_p \epsilon \sigma(\epsilon) \exp\left(\frac{-\epsilon}{T}\right), \quad (1)$$

where α_p and ϵ are the multiplicity and energy of the emitted α particles in the rest frame, T is the temperature of the source, $\sigma(\epsilon)$ is the inverse reaction cross section, and N is a normalization constant. The inverse reaction cross section

$\sigma(\epsilon)$ is calculated using the Wong's expression [19]:

$$\sigma(\epsilon) = \frac{\hbar\omega R_0^2}{2\epsilon} \ln \left(1 + \exp \left[\frac{2\pi}{\hbar\omega} (\epsilon - V_B) \right] \right), \quad (2)$$

where $\hbar\omega$ is the curvature of fusion barrier for angular momentum $\ell = 0$. The values of $\hbar\omega$ for prescission and postsission sources are determined from the fits to the fusion excitation functions for ${}^4\text{He}+{}^{237}\text{Np}$ [20] and ${}^4\text{He}+{}^{59}\text{Co}$ [21], respectively, with the predictions of the one-dimensional barrier penetration model code CCFUS [22]. Thus, $\hbar\omega_{\text{pre}}$ and $\hbar\omega_{\text{post}}$ values used in the moving source model for pre- and postsission sources are 4.8 and 4.0 MeV, respectively. The V_B is the emission barrier height of the α particles and is calculated using the expression [23];

$$V_B = \frac{1.44 Z_P (Z_S - Z_P)}{r_0 [A_P^{1/3} + (A_S - A_P)^{1/3}] + \delta} \text{MeV}, \quad (3)$$

where A_P , Z_P and A_S , Z_S are the mass and charge of the α particle and emitting source, respectively. The value of r_0 is taken to be 1.45 fm [1]. δ is a factor which takes into account for the reduction in emission barrier due to deformation effects and it is taken to be 2.0 for compound nucleus [23] and 0.4 for fission fragment [5,24]. Thus, the effective emission barrier heights (V_B) calculated for the compound nucleus and fission fragment are 20.2 and 13.4 MeV, respectively. The temperatures T_{pre} and T_{post} are calculated using the relation $T = \sqrt{E^*/a}$, where E^* is the intrinsic excitation energy of the source and a is the level-density parameter taken as $A/11$ for compound nucleus and $A/7$ for fission fragments [1]. T_{pre} is scaled down by a factor of 11/12 to account for multistep evaporation [1,25,26]. Thus, T_{pre} and T_{post} values are calculated to be 1.2 and 1.25 MeV, respectively. The energy and angular distributions for NSE are assumed to be Gaussian in the rest frame as given by the expression [1];

$$n(\epsilon, \theta) \sim \alpha_{\text{nse}} \exp \left[\frac{-(\epsilon - \epsilon_p)^2}{2\sigma_\epsilon^2} \right] \exp \left[\frac{-(90^\circ - \theta)^2}{2\sigma_\theta^2} \right], \quad (4)$$

where α_{nse} , ϵ_p , θ , σ_ϵ , and σ_θ are the α -particle multiplicity of near-scission emission, peak (or mean) energy, relative angle of α particles with respect to the scission axis, standard deviations of the energy, and the angular distributions, respectively, in the rest frame.

The α -particle spectra calculated in rest frames of four sources are converted to laboratory frames using the appropriate Jacobians and finally summed up to fit the measured spectra. In the moving source fit, the parameters T_{pre} , T_{post} , V_B^{pre} , and V_B^{post} are not varied, whereas the pre- and postsission multiplicities (α_{pre} and α_{post}) and parameters related to NSE are kept as free parameters. The mean fragment velocities are determined using Viola's systematics [27] for the total kinetic energy released in fission process. The fitted spectra for the individual source and after summing are shown in Fig. 1. The values of the parameters corresponding to the best fit are found to be $\alpha_{\text{pre}} = (5.2 \pm 0.1) \times 10^{-3}$, $\alpha_{\text{post}} = (0.17 \pm 0.02) \times 10^{-3}$, $\alpha_{\text{nse}} = (0.5 \pm 0.05) \times 10^{-3}$, $\epsilon_p = 19.3 \pm 0.3$ MeV, $\sigma_\epsilon = 3.4 \pm 0.2$ MeV, and $\sigma_\theta = 11.5^\circ \pm 1.6^\circ$, having a minimum $\chi^2/(\text{degree of freedom})$ value of 5.07. Fits are also obtained by excluding the NSE component in the moving source model

and the best-fitted values are $\alpha_{\text{pre}} = (5.8 \pm 0.1) \times 10^{-3}$ and $\alpha_{\text{post}} = (0.16 \pm 0.02) \times 10^{-3}$, corresponding to a minimum $\chi^2/(\text{degree of freedom})$ value of 6.1. Here the errors quoted in the extracted parameters include only statistical uncertainties. It is seen that fitting quality of the spectra improves particularly for $\theta_{\alpha fd} \sim 90^\circ$ if the NSE component is included in the moving source model. It should be noted here that in contrast to the works by Wilczynska *et al.* [9] for ${}^{40}\text{Ar}+{}^{232}\text{Th}$ and Lindl *et al.* for ${}^{37}\text{Cl}+{}^{124}\text{Sn}$ and ${}^{28}\text{Si}+{}^{141}\text{Pr}$ systems [6], in the the present data the small value of α_{nse} and closeness of peak energies of pre- and near-scission emission do not make the spectral shapes of $\theta_{\alpha fd} \sim 90^\circ$ differ very much from those which are away from $\theta_{\alpha fd} = 90^\circ$.

In the past, statistical model calculations with the inclusion of fission delay have been carried out to reproduce measured values of ν_{pre} and α_{pre} for various systems. In order to quantitatively understand the α_{pre} value of the present experiment, we have used the statistical model code JOANNE2 [28] which incorporates the deformation-dependent particle binding energies and transmission coefficients. Prescission emission is assumed to take place from two points in the deformation space corresponding to mean presaddle deformation (Z_{tr}) and mean saddle-to-scission deformation (Z_{ssc}). The JOANNE2 code allows only particle emission from nearly spherical systems for mean presaddle time (τ_{tr}) and then allows fission decay to compete with particle emission for mean saddle-to-scission time (τ_{ssc}). It is seen for the present system that for fixed fission delay the particle multiplicities are insensitive to Z_{tr} but very much sensitive to Z_{ssc} . Calculations are carried out by varying either Z_{ssc} or τ_{ssc} to examine its effect on ν_{pre} and α_{pre} . The value for Z_{tr} is fixed at 1.28. The value of τ_{tr} is fixed at 20 zs (1 zs = 10^{-21} s) from the systematics available in the literature [4]. In the first case, the ν_{pre} and α_{pre} values are calculated as a function of Z_{ssc} at a fixed value of $\tau_{\text{ssc}} = 100$ zs. The level-density parameters for spherical compound nucleus a_n and for the saddle-to-scission stage a_{ssc} at each Z_{ssc} are calculated within the code using the formalism of Toke and Swiatecki [29]. It is seen that ν_{pre} increases strongly with Z_{ssc} , whereas α_{pre} increases mildly up to a certain value of Z_{ssc} and then decreases as shown in Figs. 2(a) and 2(b). In the second case, the ν_{pre} and α_{pre} values are calculated as a function of τ_{ssc} at a fixed value of $Z_{\text{ssc}} = 2.23$, where α_{pre} is maximum [Fig. 2(b)]. The calculated ν_{pre} shows a strong increase with τ_{ssc} , whereas the α_{pre} increases very little initially and saturates at $\tau_{\text{ssc}} = 40$ zs as shown in Figs. 2(c) and 2(d). The shaded regions in all the panels of Fig. 2 represent the corresponding experimental values. The experimental ν_{pre} in Figs. 2(a) and 2(c) have been obtained after scaling the experimental data of Ref. [4] at $E_{\text{CN}} = 60.4$ MeV to $E_{\text{CN}} = 45$ MeV, corresponding to the present experiment. As seen from Figs. 2(a) and 2(c), the experimental ν_{pre} is reproduced with the statistical model calculation using the code JOANNE2 for suitable set of input parameters but the experimental α_{pre} cannot be reproduced by any choice of the input parameters [as seen from Figs. 2(b) and 2(d)]. Statistical model calculations using the code PACE2 [30] including fission delay are also carried and results are similar to that obtained with JOANNE2. The similar difficulty of not reproducing simultaneously experimental ν_{pre} and α_{pre} by use of a statistical

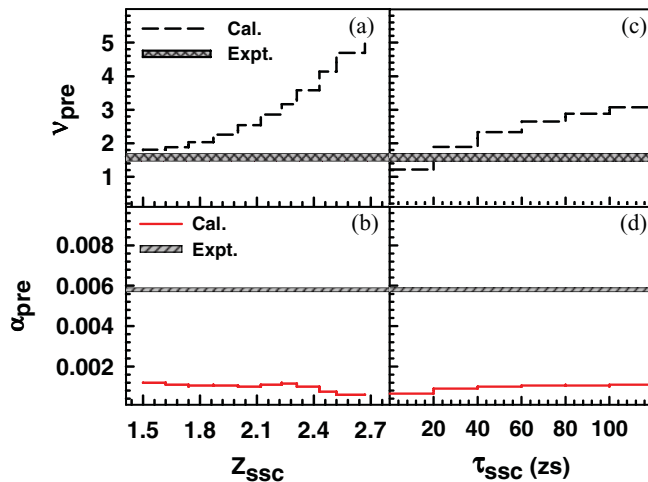


FIG. 2. (Color online) The ν_{pre} and α_{pre} calculated using the code JOANNE2 as a function of Z_{SSC} [in panels (a) and (b)] and τ_{SSC} [in panels (c) and (d)] for the $^{11}\text{B}+^{232}\text{Th}$ system. The shaded regions in all the panels represent the corresponding experimental values of ν_{pre} and α_{pre} . The experimental ν_{pre} is taken from literature (see text).

model code has been reported earlier also for the $^{28}\text{Si}+^{232}\text{Th}$ system [31].

The α_{pre} values measured earlier in many heavy-ion-induced fusion-fission reactions are observed to increase nonlinearly with an excitation energy of the compound nucleus (E_{CN}) [5]. In order to verify this nonlinear behavior of α_{pre} , statistical model calculations are carried out as a function of E_{CN} using the code JOANNE2 for many target-projectile systems. It is seen that the α_{pre} increases nonlinearly with compound nucleus excitation energy as $E_{\text{CN}}^{1.5}$ to $E_{\text{CN}}^{3.5}$ in going from compound nuclear mass number 150 to 270. Therefore, with a proper scaling of α_{pre} by a certain power of E_{CN} , it is possible to obtain a systematic behavior with respect to the α -particle emission Q value for different target-projectile systems leading to a wide variety of compound nuclei. The experimental values of α_{pre} normalized with E_{CN}^n for all available data for various systems are plotted as a function of the α -particle emission Q value (Q_α) at different values of n in the range of 1.0 to 3.5. For each value of n , the normalized α_{pre} shows a linearly increasing trend with Q_α . In order to determine the best power dependence of α_{pre} on E_{CN} , the χ^2 value is determined for each n by comparing the data for normalized α_{pre} as a function of Q_α with the best linear fit to the data. The variation of χ^2 with n is obtained to be parabolic from where the best fit value of n is obtained as 2.3 ± 0.1 . Therefore, in order to compare the α_{pre} values for various systems we have normalized the available data on α_{pre} with $E_{\text{CN}}^{2.3}$. The spread in α_{pre} value after normalizing with $E_{\text{CN}}^{2.3}$ for a given system is observed to be within the error bars in cases, where the α_{pre} data are available as a function of E_{CN} [2,5,6,18]. In these cases a weighted average of the normalized α_{pre} values of a given system is taken to investigate the dependence of α_{pre} on Q_α . Figure 3 shows the present result and available data of $\alpha_{\text{pre}}/E_{\text{CN}}^{2.3}$ as a function of the α -particle emission Q value (Q_α) for various systems. In Fig. 3, the inset shows the nearly parabolic variation of the χ^2 with n . It is observed that the

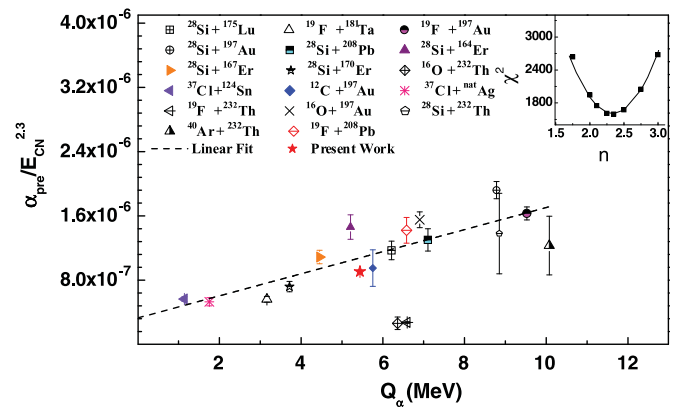


FIG. 3. (Color online) The α_{pre} normalized with $E_{\text{CN}}^{2.3}$ (E_{CN} is the compound nucleus excitation energy) as a function of the α -particle emission Q value (Q_α). The different data points are for following systems: $^{28}\text{Si}+^{175}\text{Lu}$ [1], $^{28}\text{Si}+^{164,167,170}\text{Er}$ [2], $^{37}\text{Cl}+^{124}\text{Sn}$ [6], $^{37}\text{Cl}+^{\text{nat}}\text{Ag}$ [8], $^{40}\text{Ar}+^{232}\text{Th}$ [9], $^{19}\text{F}+^{232}\text{Th}$ [18], and $^{28}\text{Si}+^{232}\text{Th}$ [31]. Data for $^{28}\text{Si}+^{197}\text{Au}$, $^{28}\text{Si}+^{208}\text{Pb}$, $^{19}\text{F}+^{197}\text{Au}$, $^{19}\text{F}+^{208}\text{Pb}$, $^{16}\text{O}+^{197}\text{Au}$, and $^{19}\text{F}+^{197}\text{Ta}$ are from Ref. [5] and for $^{16}\text{O}+^{232}\text{Th}$ and $^{12}\text{C}+^{197}\text{Au}$ are from Ref. [7]. The dashed line is a linear fit to the data. The inset shows the parabolic variation of χ^2 with the excitation energy normalization factor n (see text).

normalized α_{pre} shows a correlation with Q_α and increases linearly. The statistical theory also predicts that, for a given E_{CN} , particle emission width increases with the emission Q value [32]. It is interesting to note that the ν_{pre} values show a systematic behavior in terms of fissility after normalizing with E_{CN} [4], whereas α_{pre} shows a systematic behavior in terms of Q_α after normalizing with $E_{\text{CN}}^{2.3}$. However, it would be more relevant to analyze the ν_{pre} also in terms of the neutron emission Q value because the same fissility can be achieved for compound nuclei having widely different Q values for a given particle emission.

The value of α_{nse} determined in the present work at $E_{\text{CN}} = 45$ MeV is significantly lower than the Z^2/A systematics of low-excitation-energy fission. In low-excitation-energy fission α_{nse} increases linearly as a function of Z^2/A of the fissioning system and it is consistent with liquid-drop-model calculations for dynamical emission of α particles near the scission configuration as the gain in potential energy from saddle to scission increases with Z^2/A [11,12]. The peak energy for NSE α particles (ϵ_p) in low-energy fission is constant within 15 to 16 MeV, whereas in heavy-ion-induced fission it is scattered from 12.5 to 19.5 MeV for different systems [1,2,6–9]. In heavy-ion-induced fusion-fission reactions it has been observed that α_{nse} increases with excitation energy [2,7], in contrast to low-excitation-energy fission where dependence of the α_{nse} on excitation energy in the range of 8 to 20 MeV is quite weak [11]. These comparisons about the features of NSE indicate that the near-scission emission mechanism in heavy-ion-induced fission differs from low-excitation-energy fission.

In order to understand the near-scission emission mechanism in heavy-ion fusion-fission process, the ratio of α_{nse} to total pre-scission α -particle multiplicity ($\alpha_{\text{pre}} + \alpha_{\text{nse}}$) is calculated for the present system and other heavy-ion data

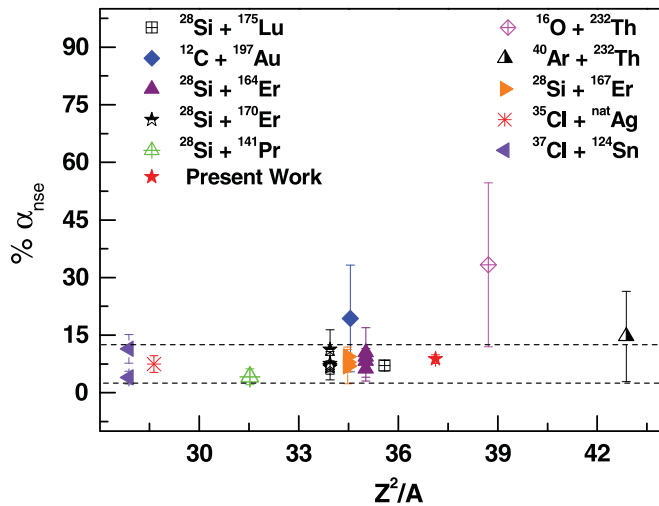


FIG. 4. (Color online) The $\% \alpha_{\text{nse}}$ as a function of Z^2/A of the fissioning system. The different data points are for following systems: $^{28}\text{Si}+^{175}\text{Lu}$ [1], $^{28}\text{Si}+^{164,167,170}\text{Er}$ [2], $^{37}\text{Cl}+^{\text{nat}}\text{Ag}$ [8], and $^{40}\text{Ar}+^{232}\text{Th}$ [9]. Data for $^{37}\text{Cl}+^{124}\text{Sn}$ and $^{28}\text{Si}+^{141}\text{Pr}$ are from Ref. [6] and for $^{16}\text{O}+^{232}\text{Th}$ and $^{12}\text{C}+^{197}\text{Au}$ are from Ref. [7]. The vertical spread in some cases corresponds to different excitation energies of a given system. The dashed lines are shown to guide the eye.

from literature. The fractional α_{nse} for the present system is determined to be $(8.6 \pm 0.2)\%$. The fractional α_{nse} for all available systems is plotted as a function of Z^2/A as shown in Fig. 4, where vertical spread in some cases corresponds to different excitation energies of a given system. It is seen that fractional α_{nse} is nearly same at around 10% of the total pre-scission multiplicity over a wide range of Z^2/A and excitation energy, as indicated with dashed lines in Fig. 4. The insensitivity of α_{nse} with Z^2/A has been seen earlier also by Sowinski *et al.* [7] for two projectile-target systems having widely different Z^2/A values. These features of α_{nse} in heavy-ion fission indicates that α particles emitted from

neck region near the scission point are due to a statistical emission process in contrast to low-energy fission where it is a pure dynamical process. It seems that as the available excitation energy increases, statistical emission dominates over dynamical emission. This indicates that the neck collapse is faster in the case of low-energy or spontaneous fission [13], whereas at higher excitation energies, it is a slow process. It may, therefore, be inferred that the nuclear collective motion exhibits a change from a superfluid to viscous nature as the excitation energy is increased. In the literature, it has been conclusively established that the α_{nse} in thermal or 1-MeV neutron-induced fission (corresponding $E_{\text{CN}} = 6\text{--}8$ MeV) is less than in spontaneous fission of the same fissioning nuclei [33–35] which is also in favor of the above arguments.

In summary, we have measured the α -particle multiplicities corresponding to different stages of emission in the fusion-fission process in the ^{11}B (62 MeV)+ ^{232}Th reaction. The present results along with data from the literature have been used to carry out a systematic analysis for α_{pre} and α_{nse} as a function of Z^2/A and excitation energy for various target-projectile systems. It is seen that α_{pre} values normalized to $E_{\text{CN}}^{2.3}$ show a systematic linearly increasing trend with α -particle emission Q value. The fraction of near-scission multiplicity is observed to be nearly the same at around 10% of the total pre-scission multiplicity for various systems over a wide range of Z^2/A and excitation energy, suggesting that the near-scission emission of α particles is a statistical process in heavy-ion-induced fission reactions. The above observation may indicate a changeover of nuclear collective motion from a superfluid to a viscous nature with increasing excitation energy.

Authors thank the operating staff of Pelletron accelerator facility for the excellent operation of the machine, R. P. Vind, A. L. Inkar, and R. V. Jangale for their help during the experiment. We are also thankful to Drs. S. S. Kapoor, Pratap Roy, Zafar Ahmed, Santanu Pal, Jhilam Sadhukhan, and Ajay Kumar for discussion on various aspects of this work.

- [1] K. Ramachandran *et al.*, *Phys. Rev. C* **73**, 064609 (2006).
 [2] J. P. Lestone, J. R. Leigh, J. O. Newton, D. J. Hinde, J. X. Wei, J. X. Chen, S. Elfstrom, and M. Z. Pfabe, *Nucl. Phys. A* **559**, 277 (1993).
 [3] M. R. Pahlavani and D. Naderi, *Phys. Rev. C* **83**, 024602 (2011).
 [4] A. Saxena, A. Chatterjee, R. K. Choudhury, S. S. Kapoor, and D. M. Nadkarni, *Phys. Rev. C* **49**, 932 (1994).
 [5] H. Ikezoe *et al.*, *Phys. Rev. C* **46**, 1922 (1992).
 [6] B. Lindl, A. Brucker, M. Bantel, H. Ho, R. Muffler, L. Schad, M. G. Trauth, and J. P. Wurm, *Z. Phys. A* **328**, 85 (1987).
 [7] M. Sowinski, M. Lewitowicz, R. Kupczak, A. Jankowski, N. K. Skobelev, and S. Chojnacki, *Z. Phys. A* **324**, 87 (1986).
 [8] L. Schad, H. Ho, G.-Y. Fan, B. Lindl, A. Pfoh, R. Wolski, and J. P. Wurm, *Z. Phys. A* **318**, 179 (1984).
 [9] K. Siwek-Wilczynska, J. Wilczynski, H. K. W. Leegte, R. H. Siemssen, H. W. Wilschut, K. Grotowski, A. Panasiewicz, Z. Sosin, and A. Wieloch, *Phys. Rev. C* **48**, 228 (1993).
 [10] W. W. Wilcke, J. P. Kosky, J. R. Birkelund, M. A. Butler, A. D. Dougan, J. R. Huizenga, W. U. Schroder, H. J. Wollersheim, and D. Hilscher, *Phys. Rev. Lett.* **51**, 99 (1983).
 [11] R. Vandenbosch and J. R. Huizenga, *Nuclear Fission* (Academic, New York, 1973).
 [12] A. K. Sinha, D. M. Nadkarni, and G. K. Mehta, *Pramana J. Phys.* **33**, 85 (1989).
 [13] I. Halpern, *Annu. Rev. Nucl. Sci.* **21**, 245 (1971).
 [14] J. P. Lestone, *Phys. Rev. C* **70**, 021601 (2004).
 [15] R. P. Vind, A. L. Inkar, R. K. Choudhury, B. K. Nayak, A. Saxena, R. G. Thomas, D. C. Biswas, and B. V. John, *Nucl. Instr. Meth. A* **580**, 1435 (2007).
 [16] D. C. Biswas, V. S. Ambekar, L. M. Pant, B. V. Dinesh, and R. K. Choudhury, *Nucl. Instr. Meth. A* **340**, 551 (1994).
 [17] Y. K. Gupta *et al.*, *Nucl. Instr. Meth. A* **629**, 149 (2011).
 [18] A. Chatterjee, A. Navin, S. Kailas, P. Singh, D. C. Biswas, A. Karnik, and S. S. Kapoor, *Phys. Rev. C* **52**, 3167 (1995).
 [19] C. Y. Wong, *Phys. Rev. Lett.* **31**, 766 (1973).
 [20] A. Fleury, F. H. Ruddy, M. N. Namboodiri, and J. M. Alexander, *Phys. Rev. C* **7**, 1231 (1973).
 [21] J. M. D'Auria, M. J. Fluss, L. Kowalski, and J. M. Miller, *Phys. Rev.* **168**, 1224 (1968).

- [22] C. H. Dasso, *Comput. Phys. Commun.* **46**, 187 (1987).
- [23] R. Yanez, T. A. Bredeweg, E. Cornell, B. Davin, K. Kwiatkowski, V. E. Viola, R. T. de Souza, R. Lemmon, and R. Popescu, *Phys. Rev. Lett.* **82**, 3585 (1999).
- [24] J. M. Alexander, D. Guerreau, and L. C. Vaz, *Z. Phys. A* **305**, 313 (1982).
- [25] E. Holub, D. Hilscher, G. Ingold, U. Jahnke, H. Orf, and H. Rossner, *Phys. Rev. C* **28**, 252 (1983).
- [26] K. J. L. Coureur and D. W. Lang, *Nucl. Phys.* **13**, 32 (1959).
- [27] V. E. Viola, K. Kwiatkowski, and M. Walker, *Phys. Rev. C* **31**, 1550 (1985).
- [28] J. P. Lestone, *Phys. Rev. Lett.* **70**, 2245 (1993).
- [29] J. Toke and W. J. Swiatecki, *Nucl. Phys. A* **372**, 141 (1981).
- [30] A. Gavron, *Phys. Rev. C* **21**, 230 (1980).
- [31] A. Saxena *et al.*, *Nucl. Phys. A* **730**, 299 (2004).
- [32] T. Ericson, *Adv. Phys.* **9**, 425 (1960).
- [33] M. Rajagopalan and T. D. Thomas, *Phys. Rev. C* **5**, 1402 (1972).
- [34] T. D. Thomas and S. L. Whetstone, *Phys. Rev.* **144**, 1060 (1965).
- [35] R. A. Noblest, *Phys. Rev.* **126**, 1508 (1962).